

Effects of nitrogen incorporation on the interfacial layer between thermally grown dielectric films and SiC

S. A. Corrêa, C. Radtke, G. V. Soares, L. Miotti, I. J. R. Baumvol, S. Dimitrijević, J. Han, L. Hold, F. Kong, and F. C. Stedile

Citation: [Applied Physics Letters](#) **94**, 251909 (2009); doi: 10.1063/1.3159812

View online: <http://dx.doi.org/10.1063/1.3159812>

View Table of Contents: <http://scitation.aip.org/content/aip/journal/apl/94/25?ver=pdfcov>

Published by the [AIP Publishing](#)

Articles you may be interested in

[The effect of dielectric confinement on photoluminescence of In₂O₃-SiO₂ nanocomposite thin films incorporated by nitrogen](#)

J. Appl. Phys. **113**, 184303 (2013); 10.1063/1.4803877

[Sequential thermal treatments of SiC in NO and O₂: Atomic transport and electrical characteristics](#)

Appl. Phys. Lett. **91**, 041906 (2007); 10.1063/1.2763966

[Effect of impurities on the fixed charge of nanoscale HfO₂ films grown by atomic layer deposition](#)

Appl. Phys. Lett. **89**, 112903 (2006); 10.1063/1.2348735

[Interfacial characteristics of N-incorporated HfAlO high-*k* thin films](#)

Appl. Phys. Lett. **84**, 5243 (2004); 10.1063/1.1764595

[Interfacial layer formation during high-temperature annealing of ZrO₂ thin films on Si](#)

Appl. Phys. Lett. **81**, 3431 (2002); 10.1063/1.1517407

A promotional banner for Applied Physics Reviews. On the left is a cover image of an Applied Physics Reviews journal issue, showing a diagram of a layered structure. The background is a blue gradient with a bright light source on the right and a molecular model of blue spheres. The text 'NEW Special Topic Sections' is prominently displayed in white. Below this, it says 'NOW ONLINE' in yellow, followed by 'Lithium Niobate Properties and Applications: Reviews of Emerging Trends' in white. The AIP Applied Physics Reviews logo is in the bottom right corner.

NEW Special Topic Sections

NOW ONLINE
Lithium Niobate Properties and Applications:
Reviews of Emerging Trends

AIP Applied Physics Reviews

Effects of nitrogen incorporation on the interfacial layer between thermally grown dielectric films and SiC

S. A. Corrêa,^{1,a)} C. Radtke,¹ G. V. Soares,² L. Miotti,^{2,3,b)} I. J. R. Baumvol,^{2,3} S. Dimitrijević,⁴ J. Han,⁴ L. Hold,⁴ F. Kong,⁴ and F. C. Stedile¹

¹Instituto de Química, Universidade Federal do Rio Grande do Sul, 91509-900 Porto Alegre, Brazil

²Centro de Ciências Exatas e Tecnologia, Universidade de Caxias do Sul, Caxias do Sul 95070-560, Brazil

³Instituto de Física, Universidade Federal do Rio Grande do Sul, 91509-900 Porto Alegre, Brazil

⁴Queensland Microtechnology Facility and Griffith School of Engineering, Griffith University, Nathan, Queensland 4111, Australia

(Received 13 March 2009; accepted 6 June 2009; published online 26 June 2009)

C-containing interlayers formed between the SiC substrate and dielectric films thermally grown in O₂, NO, and in O₂ followed by annealing in NO were investigated. X-ray reflectometry and x-ray photoelectron spectroscopy were used to determine N and C incorporation in dielectric films and interlayers, as well to determine their mass densities and thicknesses. The thickest C-containing interlayer was observed for films thermally grown in O₂, whereas the thinnest one was observed for films directly grown in NO, evidencing that the presence of N decreases the amount of carbonaceous compounds in the dielectric/SiC interface region. © 2009 American Institute of Physics.

[DOI: 10.1063/1.3159812]

Silicon carbide (SiC) is a wide band gap semiconductor whose properties make it very convenient as the starting material to build electronic devices for high-power, high-temperature, and/or high-frequency applications. As an additional advantage, a SiO₂ film can be thermally grown on SiC, similarly to Si, allowing the use of fabrication technology of Si-based metal-oxide-semiconductor (MOS) devices. However, SiO₂/SiC-based MOS devices present higher interface state density (D_{it}) and lower channel mobility than those typically found in SiO₂/Si-based ones.¹ This has been mainly attributed to the presence of carbonaceous compounds in the oxide near the SiO₂/SiC interface besides Si and/or C dangling bonds and suboxides.¹⁻⁴ Postoxidation annealing in N-containing atmospheres, especially in nitric oxide (NO), was reported to be an effective route to improve the electrical characteristics of the interface in SiC-based MOS structures.⁴⁻⁶ However, physicochemical and electrical modifications induced by the presence of nitrogen in SiO₂ films thermally grown on SiC (SiO_xN_y/SiC) still need to be better understood, in order to improve the electrical characteristics of this interface toward satisfactory figures.

The present work reports mainly x-ray reflectometry (XRR) and x-ray photoelectron spectroscopy (XPS) investigation of the mechanisms underlying the improvement of the electrical characteristics of SiO_xN_y/SiC structures.

Silicon-faced (0001) *n*-type on-axis 6H-SiC wafers were cleaned in a mixture of H₂SO₄ and H₂O₂ followed by the Radio Corporation of America process. After etching in a 5% HF aqueous solution for 1 min, samples were loaded in a quartz tube furnace. Three different routes were used to grow dielectric films on 6H-SiC. SiO₂ films were grown at 1100 °C for 1 h in a 100 mbar static atmosphere of O₂ isotopically enriched to 97% in ¹⁸O (¹⁸O₂-route). Direct oxynitride film growth in NO (NO-route) or NO-annealing of

Si ¹⁸O₂/SiC (¹⁸O₂/NO-route) were performed at 1175 °C for 2 h at a NO flow rate of 1 slm. The ¹⁸O enrichment of the O₂ gas (natural abundance of ¹⁸O is 0.2%) allows distinguishing it from O incorporated in the films during air exposure and/or NO annealing. ¹⁸O quantification was accessed by nuclear reaction analysis (NRA),⁷ using the ¹⁸O(*p*, α)¹⁵N reaction in the plateau of the cross section curve around 730 keV. The areal density of ¹⁶O was determined by Rutherford backscattering spectrometry in channeled geometry (c-RBS) at 2.0 MeV.⁷ Oxygen areal densities were converted into SiO₂ thicknesses using the relationship 10¹⁵ O cm⁻² = 0.226 nm of SiO₂ obtained from the 2.21 g cm⁻³ dense SiO₂.⁷ XPS analyses were performed in an Omicron-SPHERA station, using Mg *K*α radiation (1253.6 eV) at two different detection angles with respect to the normal to the sample surface: 0° (bulk sensitive mode) and 73° (surface sensitive mode). HF etching of films was performed prior to XPS analyses to reduce their thicknesses to values ~7 nm, more suitable to be probed by this technique. All spectra were fitted assuming a Shirley background. In the spectra shown below the background was already subtracted. XRR analyses were performed in a Shimadzu XRD 6000 equipment using Cu *K*α₁ radiation (λ = 1.5418 Å) and scanning in 0.02° steps. Data simulations were performed using the Parratt formalism for reflectivity.⁸

XRR results for the three different routes are shown in Fig. 1. Data obtained from the sample prepared in the ¹⁸O₂-route were simulated with two different approaches. A single-layer model, assuming only a SiO₂ film on SiC or a two-layer model, consisting of an interfacial layer of silicon oxycarbides (SiO_xC_y) between the SiO₂ film and the SiC substrate. ¹⁸O areal density determined by NRA (45 × 10¹⁵ ¹⁸O cm⁻²) was converted to SiO₂ thickness (10.2 nm, using the above relation) and used as the initial input in the simulation of XRR measurements. The simulation with the single-layer (SiO₂/SiC) model [dashed line in Fig. 1(a)] was in very poor agreement with experimental data, even after allowing the mass density of the SiO₂ film to vary in the

^{a)}Electronic mail: silma@iq.ufrgs.br.

^{b)}Present address: Department of Physics, North Carolina State University, Raleigh, NC 27695-8202, USA.

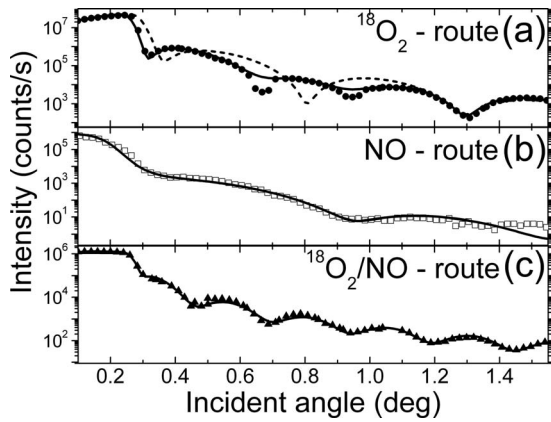


FIG. 1. XRR data from 6H-SiC samples prepared according to (a) $^{18}\text{O}_2$ -route: experimental data (solid circles), simulation with a 9 nm SiO_2 film on a 2.9 nm SiO_xC_y interfacial layer (solid line), and simulation with a 10 nm SiO_2 film without the SiO_xC_y layer (dashed line); (b) NO-route: experimental data (open squares) and simulation with a 6.5 nm SiO_xN_y film on a 1.2 nm SiO_xC_y interfacial layer (solid line); and (c) $^{18}\text{O}_2/\text{NO}$ -route: experimental data (solid triangles) and simulation with a 16 nm SiO_xN_y film on a 1.7 nm SiO_xC_y interfacial layer (solid line).

2.10–2.30 g cm^{-3} range, the roughness between 0 and 7 nm, and with unconstrained values of thicknesses. On the other hand, the assumption of a two-layer model [solid line in Fig. 1(a)], with a 2.9 nm thick interfacial layer of mass density 2.75 g cm^{-3} [between the SiO_2 film value ($\sim 2.20 \text{ g cm}^{-3}$) and that for bulk 6H-SiC (3.21 g cm^{-3})], led to a much better agreement. Roughness values were 1 nm for the interface between the SiC and the interfacial layer and 1.2 nm between the SiO_2 film (9 nm thick, mass density 2.10 g cm^{-3}) and the interfacial layer. Therefore, the total thickness determined by XRR was 11.9 nm, being in reasonable agreement with that obtained by NRA. The discrepancy between both values is attributed to the approximation made assuming the 2.21 g cm^{-3} density for the film, which is absolutely valid only for pure SiO_2 films thermally grown on Si. Since good agreement between experimental and simulation data was achieved with a two-layer model, other models with larger numbers of layers were not employed. The thickness of this interfacial layer determined from the simulation of the XRR data is consistent with previous observations^{9,10} using different analytical techniques. Thus, the two-layer model was chosen in the simulation of this sample. It corroborates the existence of a C-containing layer between the thermally grown SiO_2 film and the SiC substrate.^{2,11–13}

In order to simulate XRR data obtained from samples prepared in the NO- and $^{18}\text{O}_2/\text{NO}$ -routes, a two-layer model was also assumed, this time considering that N was incorporated in the SiO_2 film. The sum ($^{18}\text{O} + ^{16}\text{O}$) of areal densities of ^{18}O , incorporated mainly during oxidations in $^{18}\text{O}_2$ and determined by NRA, and ^{16}O , incorporated mainly during annealings in natural NO and determined by c-RBS, were 33×10^{15} and $71 \times 10^{15} \text{ O cm}^{-2}$ for NO- and $^{18}\text{O}_2/\text{NO}$ -routes, respectively. They were converted to films thicknesses (7.5 and 16 nm, respectively, using the above relation) and used as initial inputs in XRR simulations. Although small amounts of N may be present in the interfacial layer, no significant modification in the simulated reflectivity was observed when they were added. Thus, mass density of the interfacial layer was fixed at 2.75 g cm^{-3} and its thickness was allowed to vary in the 1–3 nm range, while the

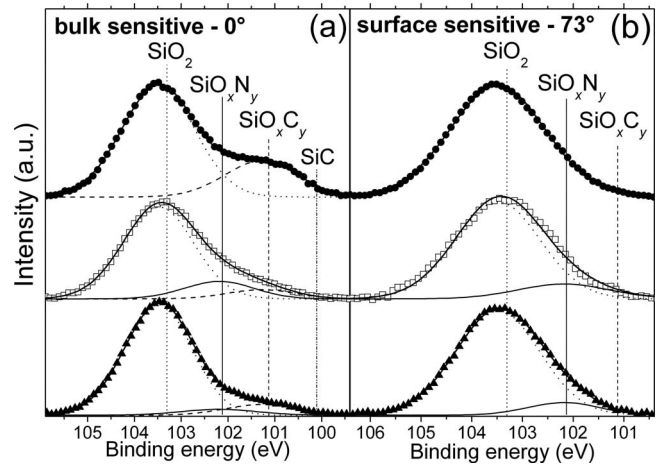


FIG. 2. Si 2p photoelectron spectra (a.u.=arbitrary a.u.units) at take-off angles of 0° [bulk sensitive (a)] and 73° [surface sensitive (b)] for 6H-SiC samples prepared according to: $^{18}\text{O}_2$ - (solid circles), NO- (open squares), and $^{18}\text{O}_2/\text{NO}$ - (solid triangles) routes. The energy positions for the Si bonding in different environments are indicated. The components used in fittings and their sum are also shown.

roughness was fixed at 1 nm between the SiC and the interfacial layer and at 1.2 nm between the interfacial layer and the dielectric film. This approach led to good fits, as shown in Figs. 1(b) and 1(c). Mass densities obtained from the XRR simulation stand for an average value for the given layer, while in fact a gradual profile of N has been identified^{11,14} for $\text{SiO}_x\text{N}_y/\text{SiC}$ structures. N-containing SiO_2 films grown in the NO- and $^{18}\text{O}_2/\text{NO}$ -routes were denser than the SiO_2 ones, with average mass densities of 2.70 and 2.45 g cm^{-3} , respectively. Films thicknesses determined by XRR (7.7 and 17.7 nm for NO- and $^{18}\text{O}_2/\text{NO}$ -routes, respectively) are close to those determined by NRA and RBS, the discrepancy being attributed to the same reason mentioned above in the case of the ^{18}O -route sample. It is noteworthy that in the NO-route, the silicon oxycarbide layer thickness is 1.2 nm, which is about half of the thickness observed for the interfacial layer for the film grown in the $^{18}\text{O}_2$ -route. This indicates that thermal growth in NO atmosphere leads to the formation of a thinner C-containing layer near the interface than films thermally grown in O_2 atmosphere, in agreement with previous results obtained from samples NO annealed following wet oxidation.¹⁵ Since the majority of electrically active defects of the dielectric/SiC interface were attributed to residual carbon, one could expect to obtain superior electrical characteristics for MOS structures prepared in the NO than for those prepared in the $^{18}\text{O}_2$ -route, consistent with previous results.^{16,17} In the $^{18}\text{O}_2/\text{NO}$ -route, the thermal oxynitridation step in NO led to a smaller reduction in the interfacial layer (1.7 nm thick) than the NO-route, justifying the fact that the best C-V characteristics observed so far for such routes¹⁷ are for capacitors prepared using the NO-route.

X-ray photoelectrons spectra from Si 2p regions are shown in Fig. 2 for bulk (a) and surface (b) sensitive modes for samples prepared according to the three different growth routes. For the $^{18}\text{O}_2$ -route (solid circles), a single component was identified in the surface sensitive mode, assigned to Si–O bonding in SiO_2 . Vertical lines correspond to the position in binding energy of the Si 2p_{3/2} components. In the bulk sensitive mode, a second component was also observed at a binding energy (E_b) 2.2 eV lower than the Si–O compo-

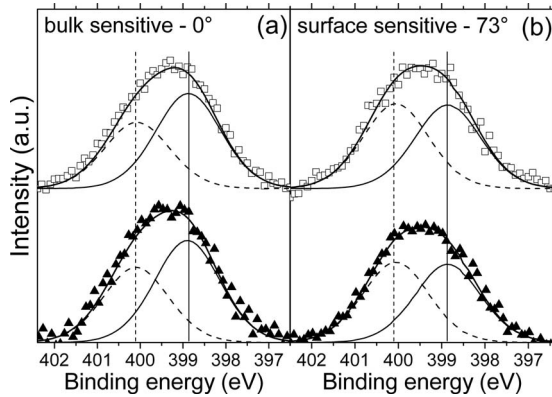


FIG. 3. N $1s$ photoelectron spectra (a.u.=arbitrary units) at take-off angles of 0° [bulk sensitive (a)] and 73° [surface sensitive (b)] for 6H-SiC samples prepared according to NO-(open squares) and $^{18}\text{O}_2$ /NO-(solid triangles) routes. The energy positions for N in a SiO_xN_y environment (higher E_b) and to N-C bonds (lower E_b) are indicated. The components used in fittings and their sum are also shown.

ment, which can be assigned to SiO_xC_y bonding in the interfacial layer^{18,19} corroborating XRR results. For the NO-(open squares) and $^{18}\text{O}_2$ /NO- (solid triangles) routes, a third component was observed, laying between those corresponding to SiO_2 and SiO_xC_y bondings, which was assigned^{6,19,20} to Si bonding in SiO_xN_y . This last component appears in both surface and bulk sensitive modes for the NO- and O_2 /NO-routes samples, while the component corresponding to the SiO_xC_y configuration was not visible in the surface sensitive mode, confirming the proposed model, which locates SiO_xC_y in the interface region with SiC.

N $1s$ photoelectron energy regions from samples prepared in the NO- (top) and $^{18}\text{O}_2$ /NO- (bottom) routes are shown in Fig. 3. Simulations of the experimental data were made assuming two components: one at $E_b=398.9$ eV and another one at $E_b=400.1$ eV. Since the binding energy of N $1s$ photoelectrons corresponding to stoichiometric silicon nitride (Si_3N_4) is $E_b=397.8$ eV,^{19,20} one verifies that most of the N was not incorporated as such in the present samples. The component at $E_b=400.1$ eV was assigned^{20,21} to N bonds in a SiO_xN_y environment. The component at $E_b=398.9$ eV can be assigned to N-C bonds,^{22,23} presenting a higher relative intensity in the bulk sensitive mode for both samples, which is plausible if one assumes that N partially passivates the residual carbon^{4,16,24} in the interface region. The observation of this component also in the surface sensitive mode, although with a lower relative intensity, is corroborated by previous results evidencing the presence of residual carbon in the bulk of SiO_2 films thermally grown on SiC.^{24,25}

In summary, characteristics of dielectric films thermally grown on SiC according to three different routes, namely,

$^{18}\text{O}_2$, NO, and $^{18}\text{O}_2$ /NO were investigated. The existence of an interfacial SiO_xC_y layer between the SiO_2 film grown in the $^{18}\text{O}_2$ -route and the SiC substrate was identified and its thickness and mass density were determined. The thickness of this layer was drastically reduced for films grown in the NO-route and a similar, although smaller reduction occurs in the case of the $^{18}\text{O}_2$ /NO-route sample. These results indicate that the electrical passivation effect of N incorporation comes from the decrease in carbonaceous compounds in the dielectric/SiC interface region.

The authors would like to thank MCT/CNPq, INCT, CAPES, FAPERGS, and ARC (Australian Research Council) for financial support.

- ¹V. V. Afanasev, M. Bassler, G. Pensl, and M. Schulz, *Phys. Status Solidi A* **162**, 321 (1997).
- ²B. Hornetz, H.-J. Michel, and J. Halbritter, *J. Mater. Res.* **9**, 3088 (1994).
- ³K. C. Chang, N. T. Nuhfer, L. M. Porter, and Q. Wahab, *Appl. Phys. Lett.* **77**, 2186 (2000).
- ⁴S. Dhar, L. C. Feldman, S. Wang, T. Isaacs-Smith, and J. R. Williams, *J. Appl. Phys.* **98**, 014902 (2005).
- ⁵D. Sweatman, S. Dimitrijević, H.-F. Li, P. Tanner, and H. B. Harrison, *Mater. Res. Soc. Symp. Proc.* **470**, 413 (1997).
- ⁶H.-F. Li, S. Dimitrijević, D. Sweatman, H. B. Harrison, P. Tanner, and B. Feil, *J. Appl. Phys.* **86**, 4316 (1999).
- ⁷I. J. R. Baumvol, *Surf. Sci. Rep.* **36**, 1 (1999).
- ⁸L. G. Parratt, *Phys. Rev.* **95**, 359 (1954).
- ⁹G. V. Soares, C. Radtke, I. J. R. Baumvol, and F. C. Stedile, *Appl. Phys. Lett.* **88**, 041901 (2006).
- ¹⁰T. Zheleva, A. Lelis, G. Duscher, F. Liu, I. Levin, and M. Das, *Appl. Phys. Lett.* **93**, 022108 (2008).
- ¹¹K.-C. Chang, Y. Cao, L. M. Porter, J. Bentley, S. Dhar, L. C. Feldman, and J. R. Williams, *J. Appl. Phys.* **97**, 104920 (2005).
- ¹²C. Radtke, I. J. R. Baumvol, J. Morais, and F. C. Stedile, *Appl. Phys. Lett.* **78**, 3601 (2001).
- ¹³S. A. Corrêa, C. Radtke, G. V. Soares, I. J. R. Baumvol, C. Krug, and F. C. Stedile, *Electrochem. Solid-State Lett.* **11**, H258 (2008).
- ¹⁴K. McDonald, M. B. Huang, R. A. Weller, L. C. Feldman, J. R. Williams, F. C. Stedile, I. J. R. Baumvol, and C. Radtke, *Appl. Phys. Lett.* **76**, 568 (2000).
- ¹⁵K.-C. Chang, L. M. Porter, J. Bentley, C.-Y. Lu, and J. Cooper, Jr., *J. Appl. Phys.* **95**, 8252 (2004).
- ¹⁶P. Jamet, S. Dimitrijević, and P. Tanner, *J. Appl. Phys.* **90**, 5058 (2001).
- ¹⁷G. V. Soares, I. J. R. Baumvol, L. Hold, F. Kong, J. Han, S. Dimitrijević, C. Radtke, and F. C. Stedile, *Appl. Phys. Lett.* **91**, 041906 (2007).
- ¹⁸C. Öneby and C. G. Pantano, *J. Vac. Sci. Technol. A* **15**, 1597 (1997).
- ¹⁹P. Jamet and S. Dimitrijević, *Appl. Phys. Lett.* **79**, 323 (2001).
- ²⁰J. W. Chai, J. S. Pan, Z. Zhang, S. J. Wang, Q. Chen, and C. H. A. Huan, *Appl. Phys. Lett.* **92**, 092119 (2008).
- ²¹G.-M. Rignanese and A. Pasquarello, *Phys. Rev. B* **63**, 075307 (2001).
- ²²S. Souto, M. Pickholdz, M. C. dos Santos, and F. Alvarez, *Phys. Rev. B* **57**, 2536 (1998).
- ²³B. Wei, B. Zhang, and K. E. Johnson, *J. Appl. Phys.* **83**, 2491 (1998).
- ²⁴A. Gavrikov, A. Knizhnik, A. Safonov, A. Scherbinin, A. Bagatur'yants, B. Potapkin, A. Chatterjee, and K. Matocha, *J. Appl. Phys.* **104**, 093508 (2008).
- ²⁵C. Radtke, F. C. Stedile, G. V. Soares, C. Krug, E. B. O. da Rosa, C. Driemeier, I. J. R. Baumvol, and R. P. Pezzi, *Appl. Phys. Lett.* **92**, 252909 (2008).